ACS OMEGA

Open Access

http://pubs.acs.org/journal/acsodf

Article

Fabrication and Characterization of a Bioscaffold Using Hydroxyapatite and Unsaturated Polyester Resin

Md. Kawcher Alam, Md. Sahadat Hossain, Md. Anisur Rahman Dayan, Newaz Mohammed Bahadur, Md. Aftab Ali Shaikh,* and Samina Ahmed*

Cite This: *ACS Omega* 2024, 9, 15210−15221

Read Online

ACCESS | Metrics & More | Article Recommendations

ABSTRACT: Outstanding biodegradability and biocompatibility are attributes associated with particular polyester substances that make this group useful in specific biomedical fields. To assess the potential as a biomaterial, a novel composite consisting of hydroxyapatite (HAp) and unsaturated polyester resin (UPR) was developed in this work. Using a hand-lay-up technique, various percentages (50, 40, 30, 20, and 10%) of HAp were reinforced into the UPR matrix to fabricate composite materials out of glass sheets. Prior to processing of the composite samples, hydroxyapatite was chemically synthesized in a wet chemical manner. Using a universal testing machine (UTM), Fourier transform infrared (FTIR) spectroscopy, scanning electron microscopy (SEM), and thermogravimetric analysis (TGA), the fabricated samples were characterized. The crystallographic parameters of synthesized hydroxyapatite (HAp) were also estimated through a range of formulas. The optimal amount for hydroxyapatite was 40% according to the findings of the tensile strength (TS), tensile modulus (TM), percentage of elongation at break (EB), bending strength (BS), and bending modulus (BM). Improvements in TS, TM, BS, and BM for the ideal combination were 39.39, 9.21, 912.05, and 259.96%, in each case, over the controlled one. Thermogravimetric analysis (TGA) has been implemented to determine the degradation temperature of the fabricated composites up to 600 °C.

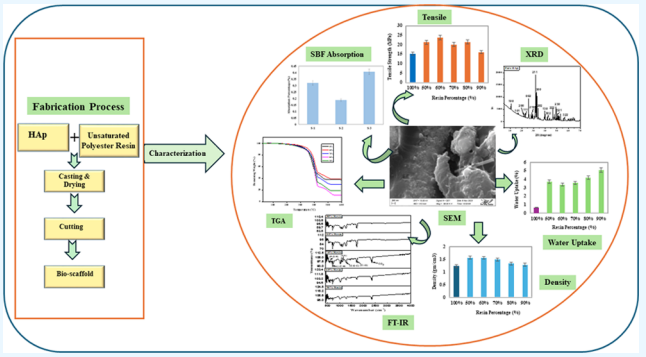

INTRODUCTION

The materials that originate from living things or utilized in body-related treatments have been referred to as "biomaterials" in different contexts.[1−3] The discipline of polymer research was initially founded on the application of polymers in biomaterials.[4,5] Large-scale arterial transplants,[6] synthetic bones,[7] hip gadgets,[8] and other long-lasting artificial body parts all depend on polymers.[9,10] Analysis is still being done to maximize the reliability and effectiveness of those substances.[11] The demands of polymers look more favorable and better adapted to the physiological requirements of the comparatively recent discipline of tissue science and engineering, where polymers are implemented to support the rebuilding of multifaceted organs.[12,13] A polymeric substance has to be considered "biocompatible" in order to serve as a substance in biomaterial applications. When the implantation of a polymeric substance inside an organ fails to result in an unfavorable response, it could easily be deemed "biocompatible".[14−16] Composite materials can be produced by combining polymers with other materials.[17,18] Hand-lay-up technique is one of the simplest ways to fabricate composite materials. During the hand-lay-up process, reinforcement and matrix are physically placed down on glass or metal sheets as blending layers.[19] Some of the instances of synthetic polymer composites are carbon fiber/epoxy resin,[20] HAp/polyethylene,[21] carbon fiber/ultra-high-molecular-weight polyethylene,[22] plant fiber/unsaturated polyester resin,[23] etc. "Avital composite" refers to a combination consisting of a reinforcement and an indispensable matrix. Composite biomaterials that are slightly resorbable, nonresorbable, and completely resorbable are additional classifications of avital composites.[24−26] The nonresorbable combinations are not meant to break down within the tissue's surroundings.[27] Extended use of implants including substitutions of joints, bone grafts, spinal tubes, plates, orthodontic care, tendons, and ligaments show the most promise for them.[28−30] A particular type of thermally and mechanically stable polymer used in composite fabrication is an unsaturated polyester resin, which mostly contains unsaturated double bonds and ester bonds through a

Received: December 1, 2023
Revised: March 3, 2024
Accepted: March 6, 2024
Published: March 20, 2024

polycondensation reaction involving unsaturated dicarboxylic acid and either saturated dicarboxylic acid or unsaturated diol.[31,32] An "unsaturated polyester resin (UPR)" is frequently reinforced with fiber materials for employment as composites. Polyesters that contain either unsaturated dicarboxylic acid and anhydride (often maleic anhydride) or saturated dicarboxylic acid and anhydride (usually phthalic anhydride) are referred to as unsaturated polyesters.[33,34] When two organic acid components combine with one or more alcohols, it forms a large polyester chain.[35] Many areas have reported the use of UPR, including composites, timber coatings, gel paints, flat layered panels, motor vehicles, washroom equipment, painting pastes, additives, stone, and fabricated concrete.[36−39] Researchers, particularly those in nations with limited resources, are currently reassessing the financial significance of polyester resins for utilizing them in the biomedical field.[40] Polyesters are used in a variety of bioresorbable surgical products, including tissue scaffolds, medication vehicles, and conventional healthcare products. Polyesters are capable of being manufactured to generate comfortable polymeric scaffolds that can substitute elastic tissues in the fields of cardiology and ophthalmology and have great physical characteristics as well as being tailored to coincide with the original tissue.[41,42] The following has been observed in the research where the rat myocardium was repaired using a polyester polymeric material.[43] Polyesters have some benefits compared to conventional orthopedic biomaterials since they are more flexible and lightweight compared to alternative biomaterials. The fact is polyesters frequently possess little harmful effect and minimizing immunological reaction is an additional benefit of employing them.[44,45] Synthesized HAp particles are recommended for utilization in implantation and replacement purposes because natively generated HAp particles fail to be stoichiometric and carry an opportunity for pathogenic progression. Though a number of synthesis processes are available, there are process variables that could work well with the wet chemical precipitation technique. Besides producing water, this process also has the notable benefit of having moderate reaction temperatures (<100 °C).[46,47] With regard to the functions of the human immune system, HAp is environmentally friendly, nonvirulent, and bioresorbable. It also possesses a remarkable capacity to stimulate bone growth and restoration. As a result, HAp has significant uses in the medical industry in areas including oral restoration, orthopedic covering, and surgeries on the spine.[48−50] While hydroxyapatite (HAp) offers literally perfect advantages as a substance for bone substitution and restoration, it also has drawbacks that make it challenging to satisfy the demands of living and medical applications due to its lack of strength, modest hardness, tricky formation, and inadequate susceptibility to fatigue in cellular conditions.[51,52] The majority of polymers lack sufficient mechanical strength and are not biocompatible. On the contrary, due to low hardness, HAp presents a challenge in making bioscaffolds by itself. So, the current study aimed to develop a novel category of composites made of a hydroxyapatite (HAp)-reinforced unsaturated polyester resin (UPR) by using the hand-lay-up technique. The physical characteristics of the resulting substances could benefit from the efficient binding properties of the resin. Studies have also been carried out to investigate a few vital characteristics of the produced composites, and these hold significance for their eventual use as biomaterials. It has been explored how the inclusion of hydroxyapatite affected the mechanical properties, morphology, thermal resistance, and water absorption characteristics of the formed composite samples. Thermogravimetric analysis (TGA), Fourier transform infrared (FTIR), universal testing machine (UTM), and scanning electron microscopy (SEM) were used to characterize the obtained materials.

MATERIALS AND METHODS

Materials. Commercial-grade $CaCO_3$ (95%) was purchased from Hatkhola, Dhaka, and the unsaturated polyester resin (industrial grade, viscosity higher than 1.0 Pa·s), and its hardener methyl ethyl ketone peroxide were purchased from the nearest market located in Gulistan, Dhaka. Each of the following chemicals seemed to be of laboratory grade and are able to be utilized without any additional purification and were purchased from E-Merck Germany: nitric acid (HNO_3), ammonium hydroxide (NH_4OH), and orthophosphoric acid (H_3PO_4) (85%). Deionized water (DI) was supplied by the Glass Research Division (GRD) of IGCRT, BCSIR, Dhaka.

Methods. *Synthesis of Hydroxyapatite (HAp).* Wet chemical synthesis of pure hydroxyapatite (HAp) has been performed by utilizing commercial calcium carbonate ($CaCO_3$) and orthophosphoric acid, H_3PO_4 (85% w/w), with a Ca/P proportion of 1.67. Equal volumes of 1.0 M H_3PO_4 solution and 1.67 M suspended $CaCO_3$ were utilized for the generation of HAp using DI water.[53] Based on specified reaction parameters (pH-10, temperature −45 °C) and constant stirring, acid was slowly introduced to the suspended solution of calcium carbonate. Once the chemical reaction was finished, the resulting product was subjected to drying at 110 °C in an oven to remove any remaining solvent. After that, the sample was smashed into fine form by employing a hand-held mortar and heated to 900 °C for 2 h.

Fabrication of the Composite. Each and every composite has been made using the hand-lay-up method. A casting was initially fabricated by placing two glass sheets on the outside of a table and covering it with a translucent and spotless plastic sheet (milot paper).[54,55] In a single plastic cup, hydroxyapatite (HAp) was employed as the reinforcing material, and the unsaturated polyester resin was employed as the matrix. HAp was incorporated in accordance with the resin percentages, which were adjusted to 50, 60, 70, 80, and 90% by weight in the composites. The mixture was thoroughly mixed with the aid of a glass rod to ensure that it was properly mixed. To make the composites, a specific amount (2%) of methyl ethyl ketone peroxide was introduced into the reinforcing and matrix constituents and thoroughly mixed. After taking care to make sure the blend contained absolutely no air bubbles, the contents of the cup were carefully and slowly placed into the milot paper, to ensure that the resin did not leak out. Next, a second piece of neat and translucent milot paper was placed on top of the blend. For 24 h, this blend was housed in glass castings. Using a hacksaw, the samples were chopped to the proper size for the mechanical, water uptake, and degradation tests.

Mechanical Properties. A universal testing machine (UTM) (M-500-30 KNCT) was used to measure the materials' tensile strength (TS), tensile modulus (TM), percentage of elongation at break (% EB), bending strength (BS), and bending modulus (BM). The starting clamp distance was set to 20 mm, and the cross-head velocity was set to 10 mm/min. The specimens were chopped to the necessary sizes (30×10 mm^2) with a hacksaw. The inspection started as soon

https://doi.org/10.1021/acsomega.3c09599
ACS Omega 2024, 9, 15210−15221

as the object being tested was fastened to the grip. Every test result was taken to be the average of a minimum of three samples.

X-ray Diffraction (XRD). Using a Rigaku SE XRD instrument, the phase and crystallographic characteristics were investigated. The operating conditions of the XRD machine were maintained at 50 mA and 40 kV, while the chiller was operated at 20−30 °C. A Cu exposure origin made Cu Kα (λ = 1.5406 Å) energy, and the XRD equipment was adjusted using an appropriate silicon reference before the samples were examined. Over a 2Θ inspection limit of 5−70°, XRD data were collected by keeping 0.01 steps when water flow rate was maintained at 4.2−4.8 L min^{-1}. Each approved set of data has been evaluated in accordance with the requirements of the ICDD database (# Card Number: 01-074-0566).

FTIR. Through the use of an IR-Prestige 21 instrument with an amplified comprehensive reflection arrangement, we determined that the functional groups of the items were determined. With a wavelength resolution of 4 cm^{-1}, 30 inspections, and a transmittance foundation based on the percentages, spectrum results ranged between 400 and 4000 cm^{-1}. A hacksaw was used for preparing the samples. To prepare the samples for FTIR analysis, they were first chopped into appropriate small sizes and then crushed into a mortar.

Thermogravimetric Analysis (TGA). The degradation properties of the produced samples was evaluated using thermogravimetric analysis (TGA) at temperatures ranging from 26.7 to 600 °C. The rate of temperature increase in TGA was 10 °C/min, and the starting weight of the specimen ranged from 500 to 800 mg. In order to keep the atmosphere inactive, nitrogen gas (N_2) was used.

Water Uptake. A hacksaw was used to cut the samples to the required weights. A total of 15 specimens were put together regarding the water absorbency analysis. After that, 15 tiny beakers were thoroughly washed, and all of them were filled with a specific volume of deionized water (DI). By employing a digital balance, the weight of the fragments was determined, and the findings were recorded. It was the initial weight of the dry samples. Next, all of the numbered samples with the control one were placed in all of the beakers containing DI water. The test fragments were immersed in DI water for 33 days in order to measure their water absorption capacity. The control and the 15 segments were taken out of the beaker after regular time intervals. The wet samples were wiped with the use of tissue paper and used to determine the weights of the fragments after water absorption. Using the weights of the dry and wet samples, the quantity and percentage of water uptake were estimated from the following equation[56]

$$\text{percentage of water uptake} = \{(\text{final weight} - \text{initial weight})/(\text{initial weight})\} \times 100 \quad (1)$$

Simulated Body Fluid (SBF). To ascertain the potential for bioactivity of the composite samples, an appropriate weight of the samples were immersed in 40 mL of SBF solution. To make simulated body fluid solution (SBF solution), proper quantities of $CaCl_2$, KCl, NaCl, Na_2SO_4, $NaHCO_3$, $K_2HPO_4 \cdot 3H_2O$, and $MgCl_2 \cdot 6H_2O$ were mixed in double distilled water and then used tris(hydroxymethyl)aminomethane and 1 M HCl solution to fix the pH (7.4) of the solution at 36.5 °C.[57] Since SBF is recognized as an unstable solution, laboratory tests were conducted with it by maintaining at chilled conditions.

Density. A density meter was used to determine the densities of the composite samples. For every percentage of the composites (50, 60, 70, 80, and 90%), two samples were considered and the mean density was calculated by adding the individual densities. Before the measurement got started, the machine was calibrated from the follow up of an appropriate procedure.

Temperature Effect. Twelve samples of the optimized percentage (60%) were cut into the proper dimensions in order to assess the stability of the composite samples at different temperature ranges. The samples were placed in the freezer and refrigerator for 4 h before the test, with the temperatures kept there at −50 and 0 °C. To evaluate strength at high temperatures, an incubator machine was also run at 50 °C for 4 h.

Effect of pH. The stability of the composite samples in various pH ranges was evaluated by cutting three samples of the optimized proportion (60%) into the appropriate sizes. The specimens were immersed in three distinct solution types, namely, pH-3, pH-7, and pH-11. Using a pH meter, nitric acid (HNO_3) and ammonium hydroxide solution (NH_4OH) were used to adjust the required solution's pH. The weights of the immersed samples were taken by using a digital balance after regular interval of 7 days, 14 days, and 21 days.

Flame Retardancy. The purpose of fire resistance testing is to evaluate how well elements execute their fire-separating qualities. A Bunsen burner was used to test the flame retardancy of the samples, and tweezers were utilized for holding milligram amounts (50−70 mg) of each sample. A stopwatch timer was employed to determine the average firing time.

Scanning Electron Microscopy (SEM). Using Phenom Pro SEM, the surface characteristics of the fabricated composites were examined. Prior to examining surface properties, each of the specimens had been coated with gold sequentially, and all pictures were acquired at a 15 kV intensifying potential. The obtained specimens were then placed on a dual-sided carbon capped test container, covered in gold, and immersed in ethanol.

RESULTS AND DISCUSSION

Phase Analysis of Synthesized Hydroxyapatite (HAp).

Crystallographic phases were verified by merging the samples that were prepared with the standard ICDD (card no. 01-074-0566) database after they underwent XRD analysis. The unique peaks of pure HAp (Figure 1) were located at d-3.43 (0 0 2), d-2.81 (2 1 1), d-2.77 (1 1 2), d-2.71 (3 0 0), d-2.62 (2 0 2), d-2.26 (1 3 0), and d-2.14 (2 2 1), in line with the typical HAp pattern. The formulas from (2) to (9) listed below can be used to determine the crystallographic parameters of the synthesized HAp, involving the lattice parameters, crystallite size, crystallinity index, crystallinity degree, microstrain, relative intensity, dislocation density, and preference growth.[58,59]

$$\text{crystallite size (using Scherrer formula)}, D = \frac{K\lambda}{\beta \cos\theta} \quad (2)$$

https://doi.org/10.1021/acsomega.3c09599
ACS Omega 2024, 9, 15210−15221

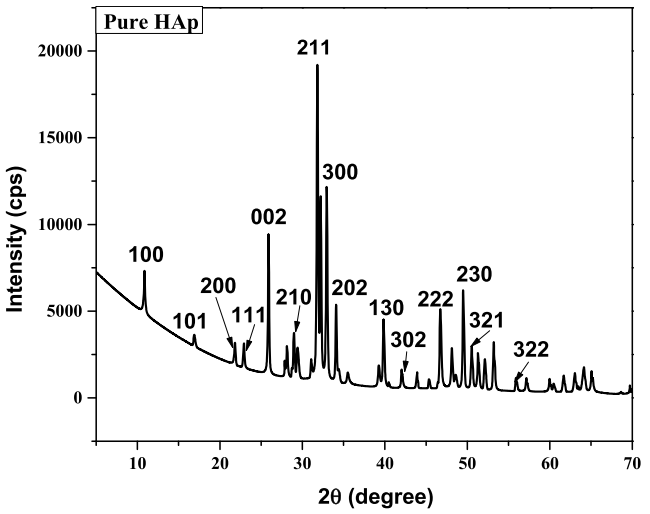

Figure 1. X-ray diffraction pattern of synthesized pure HAp.

where D = crystallite size, K = shape factor having a value of 0.90, λ = wavelength, β = FWHM (full width at half-maxima) in radian, and θ = diffraction angle (in degree).

$$\text{lattice parameter equation for hexagonal, } \left(\frac{1}{d_{hkl}}\right)^2 = \frac{4}{3}\left(\frac{h^2 + hk + k^2}{a^2}\right) + \frac{l^2}{c^2} \quad (3)$$

where d_{hkl} = interplanar distance and a, b, c, h, k, and l = lattice parameters.

$$\text{crystallinity degree, } X_c = \left(\frac{Ka}{\beta}\right)^3 \quad (4)$$

where K_a is a constant and found as a value of 0.24 for most of the HAp and β = FWHM (full width at half-maximum) in degree.

$$\text{crystallinity index, CI} = \frac{H(112) + H(300) + H(211)}{H(211)} \quad (5)$$

where H = peak heights at corresponding planes.

$$\text{dislocation density, } \delta = \frac{1}{(\text{crystallite size})^2} \quad (6)$$

$$\text{microstrain, } \in = \frac{\text{FWHM}}{4\tan(\theta)} \quad (7)$$

where FWHM is full width at half-maxima in radian and θ = diffraction angle (in degree).

Another important parameter is preference growth, determined from eq 9 by using the relative intensity of relevant planes of the prepared and standard samples. Preference growth was estimated by considering (202) with respect to (211), (112) and (300) planes.

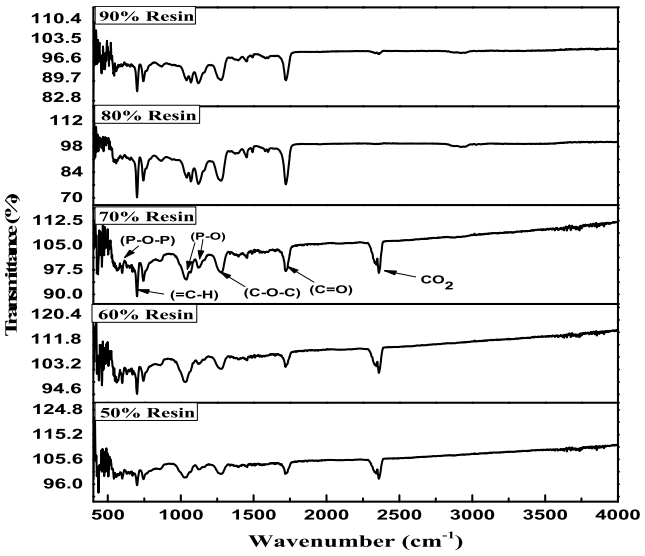

Figure 2. FTIR spectrum of HAp-reinforced unsaturated polyester resin composites.

$$\text{relative intensity, RI} = \frac{I_{(202)}}{I_{(211)} + I_{(112)} + I_{(300)}} \quad (8)$$

$$\text{preference growth, } P = \frac{\text{relative intensity}_{\text{sample}} - \text{relative intensity}_{\text{standard}}}{\text{relative intensity}_{\text{standard}}} \quad (9)$$

Table 1 provides the evidence that the crystallite size of HAp is in the nanorange and that the computed lattice characteristics closely match with those of pure HAp.[53,60] The crystals will exhibit tensile strength in relation to the internal strain of the crystal planes because of the positive microstrain. One of the most crucial crystallographic factors is preference growth, which shows whether a plane is in a thermodynamically favorable or unfavorable state. Table 1's negative preference growth indicates that the relevant plane is thermodynamically unfavorable.[60]

Determination of Functional Groups. The functional regions found in the HAp-reinforced unsaturated polyester resin composite were determined by using the technique of Fourier transform infrared spectroscopy (FTIR); the resulting spectrum is displayed in Figure 2. The carbonyl (C═O) sections in the HAp-reinforced UPR composites spectra showed a clear peak at approximately 1715 cm^{-1}, while C−O−C is an additional interesting characteristic that appears at about 1269 cm^{-1}, and ═C−H beyond plane bending was attributed to a significant peak at 700 cm^{-1}. These peaks are all distinctive peaks of the unsaturated polyester resin. Therefore, it is expected that the originally produced composite contained C−O−C and C═O groups derived from the unsaturated polyester resin. An almost identical spectrum was also described in other literature.[54,61] The sharp peak that was observed at 2350 cm^{-1} is the cause of the production of carbon

Table 1. Crystallographic Findings of Synthesized Pure HAp Nanocrystals

sample	crystal size (nm)	lattice parameters (Å)	crystallinity index (CI)	crystallinity degree (X_c)	microstrain ($\in$)	dislocation density (δ)	preference growth (P)
pure HAp	53.39	$a = b = 9.42$, $c = 6.85$	2.20	3.71	0.0023	0.35	−0.41

https://doi.org/10.1021/acsomega.3c09599
ACS Omega 2024, 9, 15210−15221

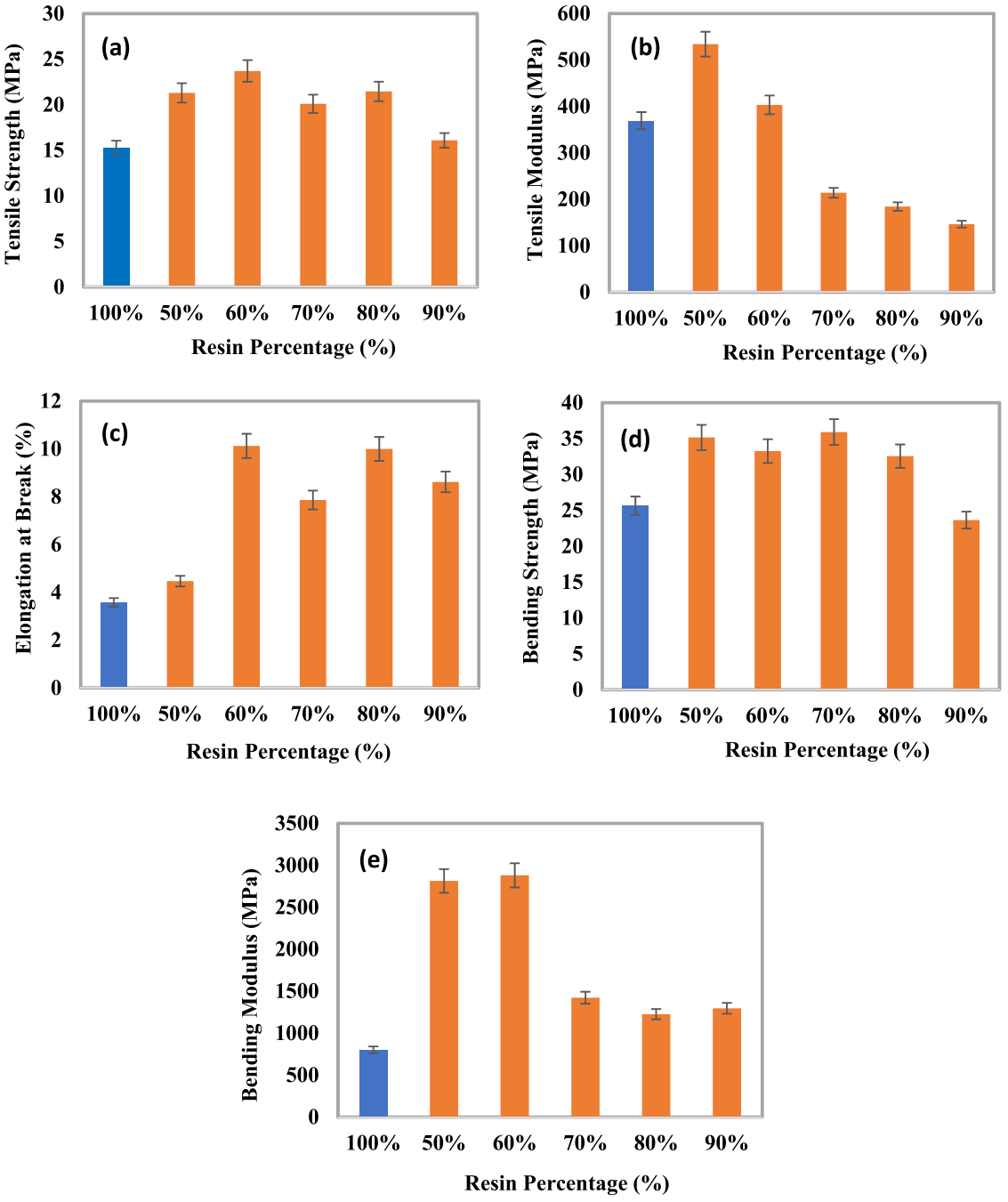

Figure 3. Variation of mechanical properties with the percentage of the unsaturated polyester resin. (a) Tensile strength, (b) tensile modulus, (c) elongation at break, (d) bending strength, and (e) bending modulus.

dioxide (CO_2) for 50, 60, and 70% resin loading. The peak that was seen at 2350 cm^{-1} is mainly the cause of naturally occurring CO_2 in the instrument during the analysis of the samples. The most intense spectrum of the composite material was obtained for 80% resin incorporation. The distinctive carbonyl group peak, that is caused by the existence of hydroxyapatite, is located at 1613 cm^{-1}. The phosphate stretching band P−O, one of the primary functional segments for HAp, is linked to the peaks at 1119, 1033, and 952 cm^{-1}. Similarly, the bending mode P−O−P group is responsible for the peaks at 600, 585, and 573 cm^{-1}. In other literature studies, FTIR spectra of bare HAp and bare UPR have been discussed.[54,62] Since no additional peak had been identified along with the distinctive peaks of hydroxyapatite (HAp) and the unsaturated polyester resin (UPR), there was no chemical link likely formed within these two materials. The improved physical characteristics were brought about by the engineered link between HAp and UPR.

Analysis of Mechanical Properties. Perhaps the absolute most crucial factor that determines a stuff's optimal use is its strength qualities. Due to the superior mechanical properties, the use of unsaturated polyester resins is becoming more and more common in consumer products. The tensile strength (TS), tensile modulus (TM), elongation at break (EB), bending strength (BS), and bending modulus (BM) of the formed composite materials are taken into consideration as the

https://doi.org/10.1021/acsomega.3c09599
ACS Omega 2024, 9, 15210−15221

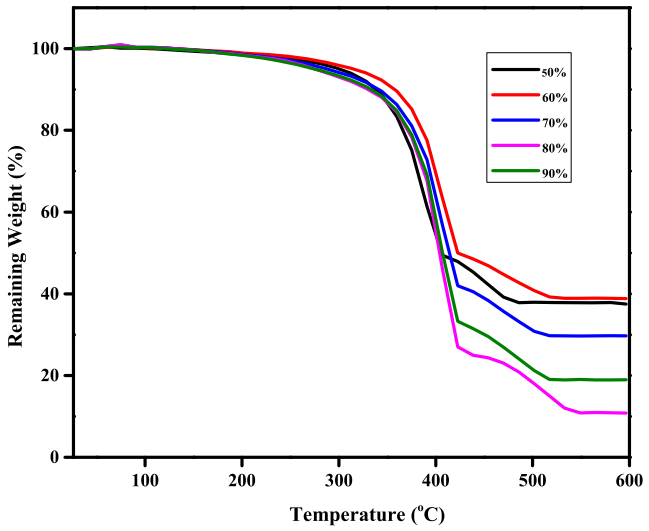

Figure 4. Weight loss of the composite samples with temperature.

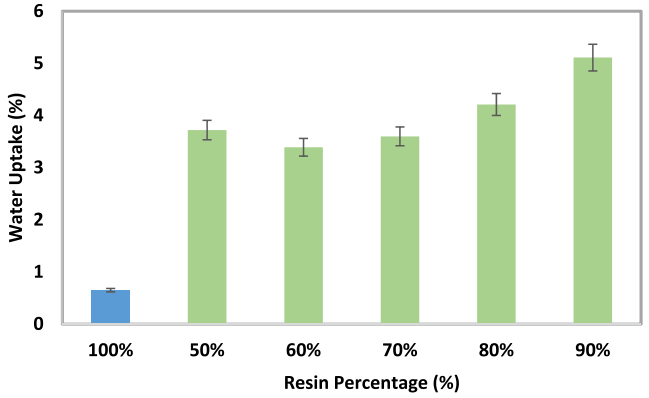

Figure 5. Water absorbency percentage of HAp-reinforced composite materials.

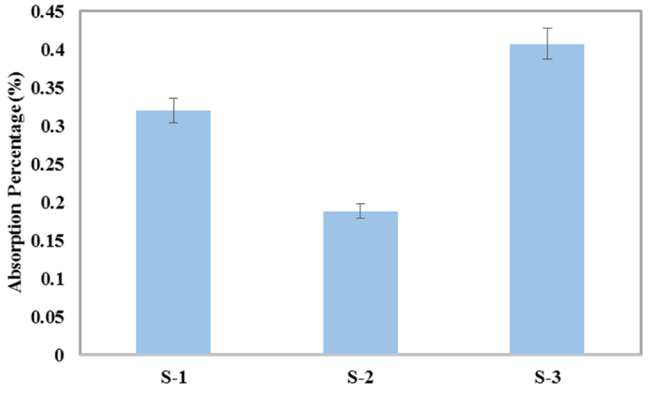

Figure 6. Absorption percentage of SBF solution for three different weights of the composite sample.

defining characteristics in this study. The results indicated that gradually the tensile strength, tensile modulus, and breaking elongation of the controlled sample are 15.28 MPa, 369.33 MPa, and 3.58%, respectively. In Figure 3a, fabricated composites exhibited an enhancement of tensile strength to 60% of the resin content. Findings of the bending and tensile measurements were gathered via the mean of three samples using a universal testing machine (UTM). Tensile properties are extremely important characteristics for any type of composite material. Insufficient adherence between the resin and HAp can lower the tensile strength of its composite. The overall results of tensile strength are displayed in Figure 3a where the data have been contrasted using the HAp-free material known as the control sample, which offers just an unsaturated polyester resin. The addition of HAp significantly increased the tensile strength (TS). The mechanical features of the materials consolidated with HAp exhibited an increase in characteristics up to a predetermined threshold, specifically 40% HAp, after which the values declined. This might occur as a result of the HAp particles' interaction with the base material, which reduced the resin's vacuum and hence enhanced the HAp and resin interaction. However, the interaction progressively diminished after surpassing a particular threshold. This results from a vacuum being filled in the resin substance's structure,[23,54,61] which causes the HAp particles to interact with one another. With regard to TM, the enhancement persisted as much as 50 percent HAp incorporation after which a progressive decline had been noted. Once more, the control produced the least force (369.33 N/mm^2), while the specimen comprising 50% HAp showed the most favorable outcome. Comparing the 50% resin-incorporating material to the control, there was a 44.57% increase percentage. Figure 3b illustrates details pertaining to the tensile modulus. In contrast, whenever the resin had been loaded, the degree of breaking elongation was upgraded. The composite material including HAp that had the most significant value, 60% resin loaded HAp, had an increase of 182.82% when compared with the control sample. The data of elongation at break are displayed in Figure 3c. The bending strength was increased by adding HAp particles to an unsaturated polyester resin. Figure 3d displays the results in a series of columns. That is clear regarding the result that the materials with 70% resin loading had the best bending strength (35.91 N/mm^2), which was 786.53% larger than the control. Composite materials are unable to get strong enough at minimal HAp amounts (10%), and conveyance of stress becomes problematic at greater percentages of the resin (90% and higher). Figure 3e shows the effect of HAp on the bending modulus of the prepared composites. The best bending modulus value was reported by the 60% resin-based material, that was 259.91% bigger compared to that of the control. When inorganic elements or unused chicken feathers are added to the unsaturated polyester resin, nearly same mechanical characteristics (TS, TM, BS, and BM) have been observed.[54,63]

Thermogravimetric Analysis of the Composites. The change of physical and chemical properties with temperature has been assessed using the method of thermogravimetric analysis (TGA). The initial reading was 26.7 °C at the beginning and 600 °C at the end. Three samples for each percentage were subjected toward the TGA evaluation. The results of the experiments for which TGA plots have been generated are shown in Figure 4. In other literature studies, TGA graphs of bare HAp and bare UPR have been shown.[54,64,65] Employing a 500 mg composite in an operating temperature that varies from 26.7 to 600 °C at a heating speed of 10 °C/min, under an inactive nitrogen environment, the process has been used to forecast materials' thermal resistance. The incorporation of a strengthening substance to the resin matrix resulted in a reduction of its thermal stability; alongside an identical effect was observed upon an inclusion of filler.[54] Around 135 °C, composites are able to maintain 99% of their integrity, and up to 350 °C, the percentage of weight loss was

https://doi.org/10.1021/acsomega.3c09599
ACS Omega 2024, 9, 15210−15221

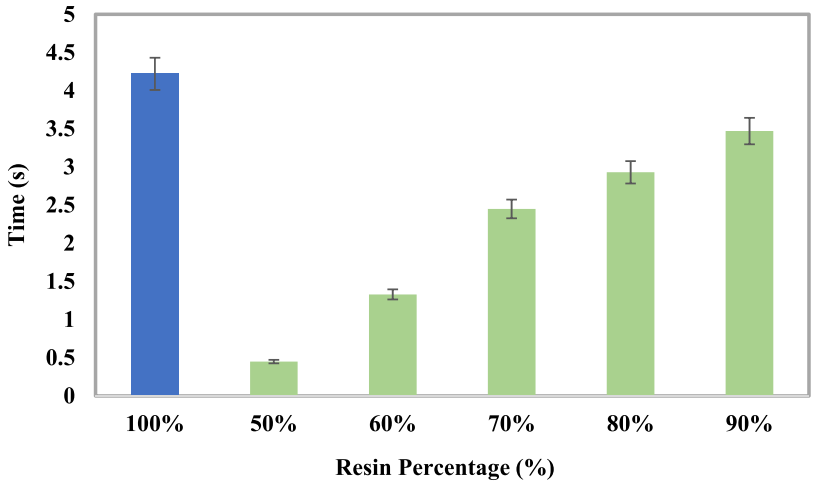

Figure 7. Illustration depicting the samples' mean firing times.

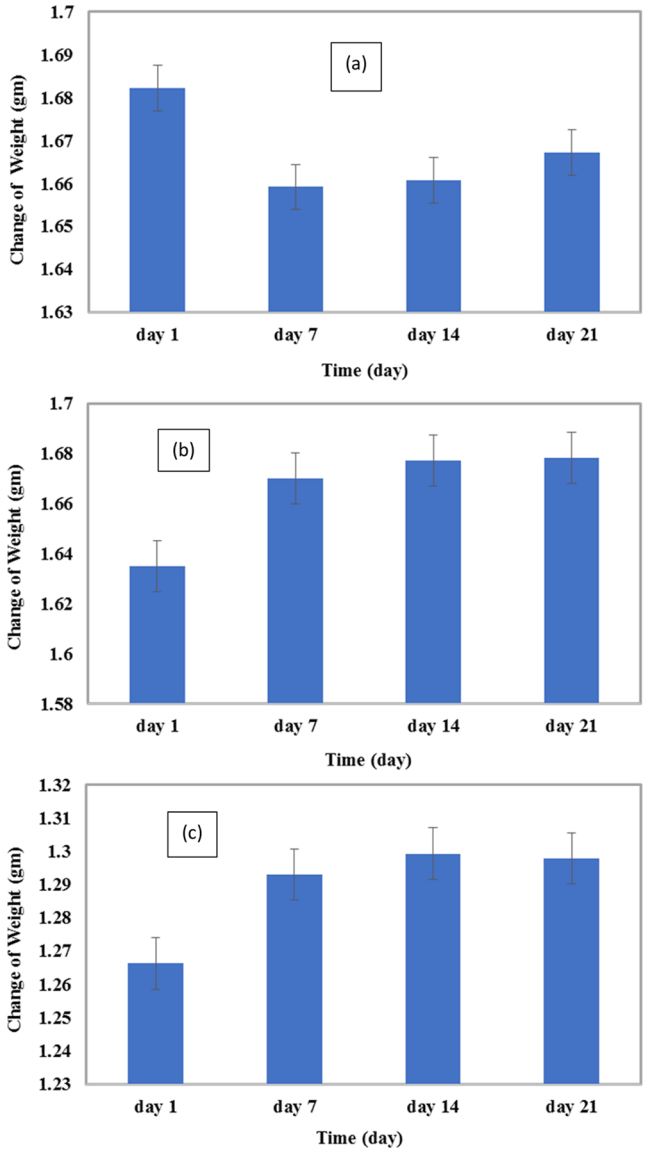

Figure 8. Change of weight at different pH ranges: (a) pH = 3, (b) pH = 7, and (c) pH = 11.

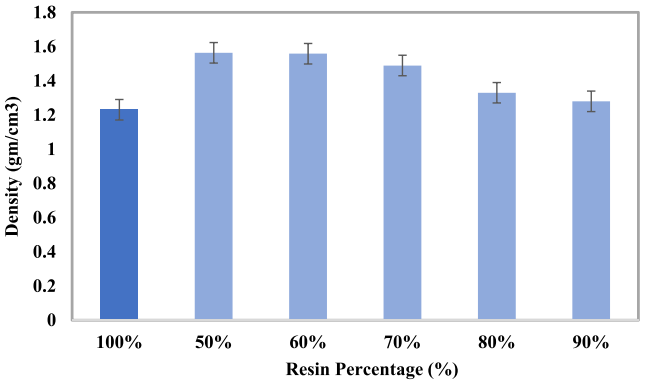

Figure 9. Density of hydroxyapatite-reinforced unsaturated polyester resin-based composites.

not too high. After that, there is a noticeable sharp decline that lasts until 420 °C. After that, as an emergence of char was occurred, fast loss has been noticed when temperatures ranged between 360 and 420 °C. The following char, along with a spotted 85% reduction in weight, has been triggered by the unsaturated polyester resin rupturing, producing polyester and polystyrene along with anhydride, CO, and CO_2. 10−15 percent of the material's weight was lost due to char deterioration, which caused a modest decrease in weight from 420 °C to the ultimate temperature.

Test for Water Uptake. Figure 5 displays the details of water absorption insights for each of the produced. For the purpose of assessing the water uptake, the composites, as well as control objects, are submerged in deionized water. The quantity of water picked up is calculated after a predetermined amount of duration. For every combination, three evaluations took place, while the mean percentages from each type were recorded. Figure 5 presents the water absorption results toward the amount of resin percentage at the ambient conditions. Based on the aforementioned result, it appears that the combination that underwent 90% resin treatment exhibited the maximum water uptake, while the control sample demonstrated the least amount of water uptake. The proportion of liquid in the materials went up with time, reaching its highest possible amounts in 4 weeks. The combinations exhibited a variation in retention of water from 3.18 to 5.40% with the variation of resin percentage, surpassing the value found in the

https://doi.org/10.1021/acsomega.3c09599
ACS Omega 2024, 9, 15210−15221

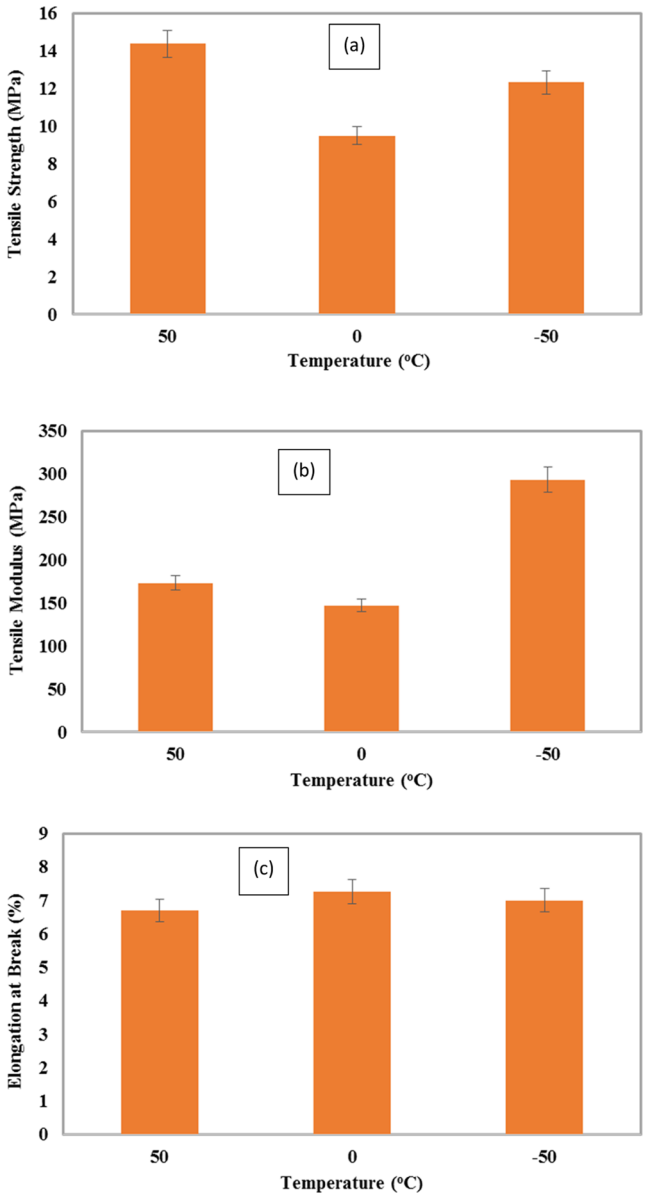

Figure 10. Temperature effect on mechanical properties of the HAp-unsaturated polyester resin composite. (a) Tensile strength (TS), (b) tensile modulus (TM), and (c) elongation at break (EB).

control item. The addition of HAp can boost the material's empty spaces, potentially leading to a greater uptake of water.[66] As unsaturated polyester resins tend to be water-resistant, there has been limited water absorbency. The development associated with the UPR phase around the HAp particles in the HAp−resin combination additionally showed modest water uptake characteristics. The water got lodged through a number of the spaces that were still present on the HAp and resin boundaries, resulting in enhanced water uptake.

Simulated Body Fluid (SBF) Test. The SBF solution was added to the optimized composite samples (60% resin), which were then kept between 5 and 10 °C. After the specified intervals of 3 days, 1 week, 2 weeks, 3 weeks, and 4 weeks, each specimen was removed and allowed to dry for 3−4 h at room temperature. Figure 6 displays how the weight in the SBF solution changed due to the absorption of SBF after a time period of 28 days.

Flame Retardancy Analysis. The flame retardancy evaluation was performed for each percentage of composite, and the results are shown in Figure 7. The sample treated with 10% HAp had the maximum firing time of 3.47 s, while the composite sample treated with 50% HAp had the shortest mean average firing time of 0.45 s. The addition of reinforcing agents results in a reduction of mean firing duration.

Effect of pH. The effects of alkali and acid on hydroxyapatite-reinforced unsaturated polyester resin-based composites were investigated for 3 weeks using varying pH levels. The results are demonstrated in Figure 8. Aqueous solutions of sodium hydroxide (NaOH) and nitric acid (HNO_3) had been utilized for the alkali and acid tests, respectively. In an acidic solution, the highest rate of reduction in weight was observed to be roughly 0.91%, this could be the result of degradation of some matrix from the composite structure. The weight of the composite samples increases slowly in the case of alkali and neutral medium after a certain amount of time. Gradual amounts of weight growth could be an indication of solution being trapped within the composites' spaces.

Density Measurement. The impact of hydroxyapatite inclusion on the density of the materials is shown in Figure 9. Since the typical density of hydroxyapatite is larger than that of the unsaturated polyester resin, the density rises with an increase in HAp addition, and identical issues with other composites have been pointed out.[67,68] The substance with no HAp has a density of 1.28 g/cm^3, and the product with 50% HAp reinforcement has the maximum density, 1.5638 g/cm^3. HAp facilitates the mass per volume of the composite sample by influencing the interaction between the matrix and the reinforcing ingredient. However, as the manufactured product contained voids, its measured density was somewhat lower than its true density. The control sample showed nearly identical results and the addition of reinforcement increased densities.[69]

Effect of Temperature on Mechanical Properties. Figure 10 shows the impact of various temperature environments (50, 0, and −50 °C) on the mechanical properties of the specimens of composites. The optimized percentage of the 60% unsaturated polyester resin was taken into consideration when conducting the test. The tensile modulus value climbed to 293.25 MPa when the temperature of the materials was lowered to −50 °C, but the percentage of elongation at break reduced to 7.001%. The intermolecular entanglement force intensified at temperatures below zero due to a substantial decrease in the vibrational motions of the combined components. At low temperatures, physical properties were substantially enhanced, while the attraction effect climbed. The tensile modulus experienced nearly 66% less at 50 °C compared to that when measured at −50 °C. Under elevated temperatures, the tensile modulus dropped as a consequence of a rise in both the rotational and vibrational oscillation of molecules caused by the change in temperature.

SEM Analysis. In order to examine the hydroxyapatite and resin adherence in the composites, the fractured materials had been picked up and their morphological concepts was examined using a scanning electron microscope. Figure 11 shows electron microscopy photographs of the surface of unsaturated polyester resin composites with 50, 30, and 10% HAp reinforcement. According to the SEM pictures, several empty spaces that resulted from the integration of the HAp particles were observed. Numerous research publications have

https://doi.org/10.1021/acsomega.3c09599
ACS Omega 2024, 9, 15210−15221

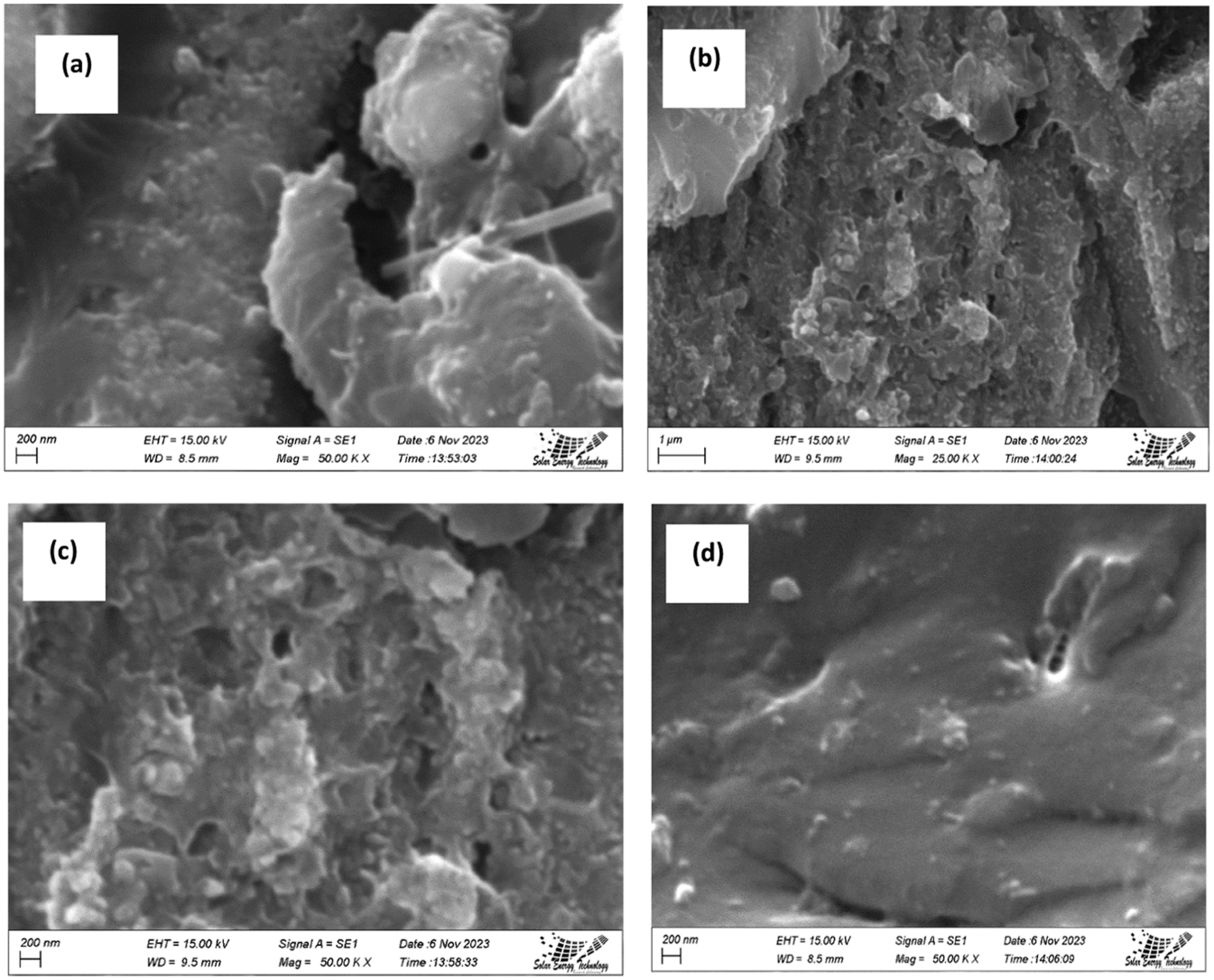

Figure 11. SEM images of HAp-reinforced unsaturated polyester resin composites; (a) 50% resin, (b, c) 70% resin, and (d) 90% resin.

reported on these kinds of holes in SEM pictures.[38,40] The fact that the HAp and matrix were tightly linked together provides convincing evidence that the composites' physical characteristics are only slightly better than those of the standard sample. There were not as many vacant spaces at a low HAp loading percentage of 10%. When 50% hydroxyapatite was added to the composite, some of the holes were easily visible. Even though there were consistently fewer vacuums in the 10% HAp scenario, the discontinuous connection and HAp particles clustering in the matrix appeared clearly in the SEM pictures.

CONCLUSIONS

An unsaturated polyester resin (UPR) and hydroxyapatite (HAp) are capable of being combined to yield composite materials that have a variety of applications as biomaterials. When using the engineered unsaturated polyester resin as the matrix, the 50% and 60% HAp-loaded composites performed ahead of the remaining percentages. 50 and 60% hydroxyapatite-reinforced unsaturated polyester resins are recommended to be utilized in place of other simply conventional reinforcement-loaded unsaturated polyester resins for biomedical purposes whenever the substantial tensile strength and bending strength of the composites need to be met. The sample made of 60% resin content and 40% HAp is more stable in comparison with other percentages, as it provides the maximum amount of tensile strength (TS) and tensile modulus (TM). For each case, the optimum combination (60%) has developments in TS, TM, BS, and BM of 39.388, 9.21, 912.05, and 259.96%, respectively, above the controlled one. The tensile modulus experienced nearly 66% less at 50 °C compared to when measured at −50 °C. FTIR and SEM images did not reveal any information regarding the chemical bonding. However, the empty areas visible in SEM images are the cause of the modest absorption of water and SBF. The pH impact indicates that the matrix from the sample's surface is degrading in an acidic condition. According to the TGA assessment of the composite samples, composites can retain 99% of their integrity up to 135 °C and after 350 °C, there is a distinct loss in integrity that continues until 420 °C. The density of bioscaffolds increases significantly as a result of HAp reinforcement.

AUTHOR INFORMATION

Corresponding Authors

Md. Aftab Ali Shaikh − *Glass Research Division, Institute of Glass & Ceramic Research and Testing, Bangladesh Council*

https://doi.org/10.1021/acsomega.3c09599
ACS Omega 2024, 9, 15210−15221

of Scientific and Industrial Research (BCSIR), Dhaka 1205, Bangladesh; Department of Chemistry, University of Dhaka, Dhaka 1000, Bangladesh; Email: aftabshaikh@du.ac.bd

Samina Ahmed − *Glass Research Division, Institute of Glass & Ceramic Research and Testing, Bangladesh Council of Scientific and Industrial Research (BCSIR), Dhaka 1205, Bangladesh; BCSIR Dhaka Laboratories, Bangladesh Council of Scientific and Industrial Research (BCSIR), Dhaka 1205, Bangladesh*; Email: shanta_samina@yahoo.com

Authors

Md. Kawcher Alam − *Glass Research Division, Institute of Glass & Ceramic Research and Testing, Bangladesh Council of Scientific and Industrial Research (BCSIR), Dhaka 1205, Bangladesh; Department of Applied Chemistry and Chemical Engineering, Noakhali Science and Technology University, Noakhali 3814, Bangladesh*

Md. Sahadat Hossain − *Glass Research Division, Institute of Glass & Ceramic Research and Testing, Bangladesh Council of Scientific and Industrial Research (BCSIR), Dhaka 1205, Bangladesh*; orcid.org/0000-0001-8273-8559

Md. Anisur Rahman Dayan − *Textile Physics Division, Bangladesh Jute Research Institute, Dhaka 1207, Bangladesh*

Newaz Mohammed Bahadur − *Department of Applied Chemistry and Chemical Engineering, Noakhali Science and Technology University, Noakhali 3814, Bangladesh*

Complete contact information is available at: https://pubs.acs.org/10.1021/acsomega.3c09599

Author Contributions

M.K.A. fabricated and characterized the hydroxyapatite-based composites, analyzed the data, and wrote the draft and original manuscript. M.S.H. conceived and designed the experiment and analyzed the data. M.A.R.D. executed the TGA analysis. N.M.B. and S.A. supervised the findings of this work. S.A. supervised the overall work and managed the required facilities.

Notes

The authors declare no competing financial interest.

■ ACKNOWLEDGMENTS

The authors are grateful to Bangladesh Council of Scientific and Industrial Research (BCSIR) authority for financial support through R&D projects (ref no. 39.02.0000.011.14.134.2021/900; date: 30.12.2021) and (ref no. 39.02.0000.011.14.157.2022/172; date: 10.11.2022). M.K.A. wishes to thank Department of Applied Chemistry and Chemical Engineering, Noakhali Science and Technology University, Noakhali, Bangladesh, for approving M.S. Thesis program.

■ REFERENCES

(1) Wang, Y.; Wang, Z.; Dong, Y. Collagen-Based Biomaterials for Tissue Engineering. *ACS Biomater. Sci. Eng.* **2023**, *9* (3), 1132−1150.

(2) Farag, M. M. Recent trends on biomaterials for tissue regeneration applications: review. *J. Mater. Sci.* **2023**, *58* (2), 527−558.

(3) Liu, S.; Yu, J. M.; Gan, Y. C.; et al. Biomimetic natural biomaterials for tissue engineering and regenerative medicine: new biosynthesis methods, recent advances, and emerging applications. *Mil. Med. Res.* **2023**, *10* (1), 16.

(4) Pires, P. C.; Mascarenhas-Melo, F.; Pedrosa, K.; et al. Polymer-based biomaterials for pharmaceutical and biomedical applications: A focus on topical drug administration. *Eur. Polym. J.* **2023**, *187*, No. 111868.

(5) Sabater i Serra, R.; Serrano-Aroca, Á. Polymer-Based Biomaterials and Tissue Engineering. *Materials* **2023**, *16*, 4923 DOI: 10.3390/ma16144923.

(6) Naegeli, K. M.; Kural, M. H.; Li, Y.; Wang, J.; Hugentobler, E. A.; Niklason, L. E. Bioengineering Human Tissues and the Future of Vascular Replacement. *Circ. Res.* **2022**, *131* (1), 109−126.

(7) Senra, M. R.; Marques, M. de F. V. Synthetic polymeric materials for bone replacement. *J. Compos. Sci.* **2020**, *4* (4), 191.

(8) Garg, T.; Sharma, G.; Shankar, S.; Singh, S. P. Tribological Performance of Polymeric Materials for Biomedical Applications. In *Assessment of Polymeric Materials for Biomedical Applications*, CRC Press: 2023; pp 121−138.

(9) Thadepalli, S. Review of multifarious applications of polymers in medical and health care textiles. *Mater. Today Proc.* **2022**, *55*, 330−336.

(10) Shahinpoor, M. *Artificial Muscles: Applications of Advanced Polymeric Nanocomposites*; CRC Press, 2021.

(11) Zhang, J.; Feng, Y.; Zhou, X.; Shi, Y.; Wang, L. Research status of artificial bone materials. *Int. J. Polym. Mater. Polym. Biomater.* **2021**, *70* (1), 37−53.

(12) Asghari, F.; Samiei, M.; Adibkia, K.; Akbarzadeh, A.; Davaran, S. Biodegradable and biocompatible polymers for tissue engineering application: a review. *Artif. Cells Nanomed. Biotechnol.* **2017**, *45* (2), 185−192.

(13) Gomes, M. et al. Natural Polymers in Tissue Engineering Applications. In *Tissue Engineering*, Elsevier, 2008; pp 145−192.

(14) Haider, A.; Haider, S.; Rao Kummara, M.; et al. Advances in the scaffolds fabrication techniques using biocompatible polymers and their biomedical application: A technical and statistical review. *J. Saudi Chem. Soc.* **2020**, *24* (2), 186−215.

(15) Asadi, N.; Del Bakhshayesh, A. R.; Davaran, S.; Akbarzadeh, A. Common biocompatible polymeric materials for tissue engineering and regenerative medicine. *Mater. Chem. Phys.* **2020**, *242*, No. 122528.

(16) Balaji, A. B.; Pakalapati, H.; Khalid, M.; Walvekar, R.; Siddiqui, H. Natural and synthetic biocompatible and biodegradable polymers. *Biodegrad. Biocompatible Polym. Compos.* **2018**, *286*, 3−32.

(17) Kijeńska, E.; Zhang, S.; Prabhakaran, M. P.; Ramakrishna, S.; Swieszkowski, W. Nanoengineered biocomposite tricomponent polymer based matrices for bone tissue engineering. *Int. J. Polym. Mater. Polym. Biomater.* **2016**, *65* (16), 807−815.

(18) Lee, S.-H.; Wang, S. Biodegradable polymers/bamboo fiber biocomposite with bio-based coupling agent. *Compos. Part Appl. Sci. Manuf.* **2006**, *37* (1), 80−91.

(19) Elkington, M.; Bloom, D.; Ward, C.; Chatzimichali, A.; Potter, K. Hand layup: understanding the manual process. *Adv. Manuf. Polym. Compos. Sci.* **2015**, *1* (3), 138−151.

(20) Li, C.-q.; Dong, H.; Zhang, W. Low-temperature plasma treatment of carbon fibre/epoxy resin composite. *Surf. Eng.* **2018**, *34* (11), 870−876.

(21) Suchanek, W.; Yoshimura, M. Processing and properties of hydroxyapatite-based biomaterials for use as hard tissue replacement implants. *J. Mater. Res.*, **1998**, *13* (1), 94−117.

(22) Reddy, T. S.; Reddy, P. R. S.; Madhu, V. Dynamic Behaviour of Carbon/Ultra High Molecular Weight Polyethylene (UHMWPE) Hybrid Composite Laminates Under Ballistic Impact. *J. Dyn. Behav. Mater.* **2021**, *7* (3), 403−413.

(23) Ali, M. F.; Hossain, M. S.; Moin, T. S.; Ahmed, S.; Chowdhury, A. S. Physico-Mechanical Properties of Treated Chicken Feather−Reinforced Unsaturated Polyester Resin Based Composites. *Nano Hybrids Compos.* **2021**, *32*, 73−84.

(24) Saad, M.; Akhtar, S.; Srivastava, S. Composite polymer in orthopedic implants: A review. *Mater. Today Proc.* **2018**, *5* (9), 20224−20231.

(25) Scholz, M.-S.; Blanchfield, J.; Bloom, L.; et al. The use of composite materials in modern orthopaedic medicine and prosthetic devices: A review. *Compos. Sci. Technol.* **2011**, *71* (16), 1791−1803.
(26) Karamuk, E.; Mayer, J.; Raeber, G. Tissue engineered composite of a woven fabric scaffold with tendon cells, response on mechanical simulation in vitro. *Compos. Sci. Technol.* **2004**, *64* (6), 885−891.
(27) Ignjatović, N.; Uskoković, D. Biodegradable composites based on nanocrystalline calcium phosphate and bioresorbable polymers. *Adv. Appl. Ceram.* **2008**, *107* (3), 142−147.
(28) Ramakrishna, S.; Mayer, J.; Wintermantel, E.; Leong, K. W. Biomedical applications of polymer-composite materials: a review. *Compos. Sci. Technol.* **2001**, *61* (9), 1189−1224.
(29) Kumar, R.; Agrawal, A. Micro-hydroxyapatite reinforced Ti-based composite with tailored characteristics to minimize stress-shielding impact in bio-implant applications. *J. Mech. Behav. Biomed. Mater.* **2023**, *142*, No. 105852.
(30) Zhao, D. S.; Moritz, N.; Laurila, P.; et al. Development of a multi-component fiber-reinforced composite implant for load-sharing conditions. *Med. Eng. Phys.* **2009**, *31* (4), 461−469.
(31) Chu, F.; Qiu, S.; Zhang, S.; et al. Exploration on structural rules of highly efficient flame retardant unsaturated polyester resins. *J. Colloid Interface Sci.* **2022**, *608*, 142−157.
(32) Hu, S.-L.; Li, Y.-M.; Hu, W.-J.; Hobson, J.; Wang, D.-Y. Strategic design unsaturated polyester resins composites with excellent flame retardancy and high tensile strength. *Polym. Degrad. Stab.* **2022**, *206*, No. 110190.
(33) Penczek, P.; Czub, P.; Pielichowski, J. Unsaturated Polyester Resins: Chemistry and Technology. In *Crosslinking in Materials Science*, Springer Berlin Heidelberg: Berlin, Heidelberg, 2005; Vol. *184*, pp 1−95.
(34) Davallo, M.; Pasdar, H.; Mohseni, M. Mechanical properties of unsaturated polyester resin. *Int. J. ChemTech Res.* **2010**, *2* (4), 2113−2117.
(35) Jones, F. R. Unsaturated Polyester Resins. In *Brydson's Plastics Materials*, Elsevier: 2017; pp 743−772.
(36) Dholakiya, B. Unsaturated polyester resin for specialty applications. *Polyester* **2012**, *7*, 167−202.
(37) Ul Haq, M. I. Applications of unsaturated polyester resins. *Russ. J. Appl. Chem.* **2007**, *80* (7), 1256−1269.
(38) Mohammad, N. A. B. Synthesis, characterization and properties of the new unsaturated polyester resins for composite applications. *MARA Univ. Technol.* **2007**, 45−56.
(39) Gao, Y.; Zhang, H.; Huang, M.; Lai, F. Unsaturated polyester resin concrete: A review. *Constr. Build. Mater.* **2019**, *228*, No. 116709.
(40) Jayabalan, M.; Shalumon, K. T.; Mitha, M. K.; Ganesan, K.; Epple, M. Effect of hydroxyapatite on the biodegradation and biomechanical stability of polyester nanocomposites for orthopaedic applications. *Acta Biomater.* **2010**, *6* (3), 763−775.
(41) Spasojević, P.; Savković, M. S. Potential of Unsaturated Polyesters in Biomedicine and Tissue Engineering. In *Applications of Unsaturated Polyester Resins*, Elsevier, 2023; 341−420.
(42) Embirsh, H. S. A.; Stajčić, I.; Gržetić, J.; et al. Synthesis, Characterization and Application of Biobased Unsaturated Polyester Resin Reinforced with Unmodified/Modified Biosilica Nanoparticles. *Polymers* **2023**, *15* (18), 3756.
(43) Zaokari, Y.; Persaud, A.; Ibrahim, A. Biomaterials for Adhesion in Orthopedic Applications: A Review. *Eng. Regen.* **2020**, *1*, 51−63.
(44) Vaishya, R.; Agarwal, A. K.; Tiwari, M.; Vaish, A.; Vijay, V.; Nigam, Y. Medical textiles in orthopedics: An overview. *J. Clin. Orthop. Trauma* **2018**, *9*, S26−S33.
(45) Chen, Q.; Zhu, C.; Thouas, G. A. Progress and challenges in biomaterials used for bone tissue engineering: bioactive glasses and elastomeric composites. *Prog. Biomater.* **2012**, *1* (1), 2.
(46) Kehoe, S. Optimisation of Hydroxyapatite (HAp) for Orthopaedic Application Via the Chemical Precipitation Technique. PhD Thesis, 2008.
(47) Mostafa, N. Y. Characterization, thermal stability and sintering of hydroxyapatite powders prepared by different routes. *Mater. Chem. Phys.* **2005**, *94* (2−3), 333−341.
(48) Irfan, M.; Irfan, M. Overview of hydroxyapatite; composition, structure, synthesis methods and its biomedical uses. *Biomed. Lett.* **2020**, *6* (1), 17−22.
(49) Oni, O. P.; Hu, Y.; Tang, S.; et al. Syntheses and applications of mesoporous hydroxyapatite: a review. *Mater. Chem. Front.* **2022**, *7*, 9−43, DOI: 10.1039/D2QM00686C.
(50) Lu, Y.; Dong, W.; Ding, J.; Wang, W.; Wang, A. Hydroxyapatite Nanomaterials: Synthesis, Properties, and Functional Applications. In *Nanomaterials from Clay Minerals*, Elsevier: 2019; pp 485−536.
(51) Ma, G. Three Common Preparation Methods of Hydroxyapatite, *IOP Conference Series: Materials Science and Engineering*, IOP Publishing: 2019; p 033057.
(52) Anandan, D.; Jaiswal, A. K. Synthesis methods of hydroxyapatite and biomedical applications: an updated review. *J. Aust. Ceram. Soc.* **2023**, 1−17, DOI: 10.1007/s41779-023-00943-2.
(53) Hossain, M. S.; Tuntun, S. M.; Bahadur, N. M.; Ahmed, S. Enhancement of photocatalytic efficacy by exploiting copper doping in nano-hydroxyapatite for degradation of Congo red dye. *RSC Adv.* **2022**, *12* (52), 34080−34094.
(54) Ali, M. F.; Ahmed, M. A.; Hossain, M. S.; Ahmed, S.; Chowdhury, A. S. Effects of inorganic materials on the waste chicken feather fiber reinforced unsaturated polyester resin-based composite: An approach to environmental sustainability. *Compos. Part C: Open Access* **2022**, *9*, No. 100320.
(55) Shokrieh, M. M.; Safari, S. Optimization of the Manufacturing Process of Natural Fibre Thermoplastic Composites in order to Minimize Warpage. *ADMT J.* **2009**, *2*, 9−15.
(56) Ali, M. F.; Hossain, M. S.; Ahmed, S.; Chowdhury, A. S. Fabrication and characterization of eco-friendly composite materials from natural animal fibers *Heliyon* 2021, *75* DOI: 10.1016/j.heliyon.2021.e06954.
(57) Chouzouri, G.; Xanthos, M. In vitro bioactivity and degradation of polycaprolactone composites containing silicate fillers. *Acta Biomater.* **2007**, *3* (5), 745−756.
(58) Sahadat Hossain, M.; Ahmed, S. Crystallographic characterization of naturally occurring aragonite and calcite phase: Rietveld refinement. *J. Saudi Chem. Soc.* **2023**, *27* (3), No. 101649.
(59) Hossain, M. S.; Uddin, M. N.; Sarkar, S.; Ahmed, S. Crystallographic dependency of waste cow bone, hydroxyapatite, and β-tricalcium phosphate for biomedical application. *J. Saudi Chem. Soc.* **2022**, *26* (6), No. 101559.
(60) Hossain, M. S.; Shaikh, M. A. A.; Rahaman, M. S.; Ahmed, S. Modification of the crystallographic parameters in a biomaterial employing a series of gamma radiation doses. *Mol. Syst. Des. Eng.* **2022**, *7* (10), 1239−1248.
(61) Hossain, M. T.; Hossain, M. S.; Kabir, M. S.; Ahmed, S.; Khan, R. A.; Chowdhury, A. S. Improvement of mechanical properties of jute-nano cellulose-reinforced unsaturated polyester resin-based composite: Effects of gamma radiation. *Hybrid Adv.* **2023**, *3*, No. 100068.
(62) Tank, K. P.; et al. FTIR, powder XRD, TEM and dielectric studies of pure and zinc doped nano-hydroxyapatite, Crystal Research and Technology. *Cryst. Res. Technol.* **2011**, *46*, 1309−1316, DOI: 10.1002/crat.201100080.
(63) Ali, M. F.; Hossain, M. S.; Moin, T. S.; Ahmed, S.; Chowdhury, A. S. Utilization of waste chicken feather for the preparation of eco-friendly and sustainable composite. *Clean. Eng. Technol.* **2021**, *4*, No. 100190.
(64) Ashok, M.; Sundaram, N. M.; Kalkura, S. N. Crystallization of hydroxyapatite at physiological temperature. *Mater. Lett.* **2003**, *57* (13−14), 2066−2070.
(65) Wang, Y.; Zhang, L.; Yang, Y.; Cai, X. The investigation of flammability, thermal stability, heat resistance and mechanical properties of unsaturated polyester resin using AlPi as flame retardant. *J. Therm. Anal. Calorim.* **2015**, *122*, 1331−1339.

(66) Al-khafaji, Z. S.; Radhi, N. S.; Mohson, S. A. Preparation and modelling of composite materials (polyester-alumina) as implant in human body. *Int. J. Mech. Eng. Technol.* **2018**, *9* (4), 468−478.
(67) Yao, F.; Wu, Q.; Lei, Y.; Xu, Y. Rice straw fiber-reinforced high-density polyethylene composite: Effect of fiber type and loading. *Ind. Crops Prod.* **2008**, *28* (1), 63−72.
(68) Lu, N.; Oza, S. Thermal stability and thermo-mechanical properties of hemp-high density polyethylene composites: Effect of two different chemical modifications. *Composites, Part B* **2013**, *44* (1), 484−490.
(69) Sapuan, S. M.; Aulia, H.; Ilyas, R.; et al. Mechanical properties of longitudinal basalt/woven-glass-fiber-reinforced unsaturated polyester-resin hybrid composites. *Polymers* **2020**, *12* (10), 2211.

https://doi.org/10.1021/acsomega.3c09599
ACS Omega 2024, 9, 15210−15221